

---

**CHAPTER 1**

**Introduction and Literature Review**

---

## 1.1. Introduction

The word “nanotechnology” is familiarized by noble laureate Richard P. Feynman during his famous speech in 1959 “There is a Plenty of Room at the Bottom”, where he demonstrated about the world in which atoms could be manipulated at an enormously small scale i.e., the nanoscale [Feynman (1960)]. The term Nanotechnology was given by Professor Norio Taniguchi [Handy *et al.* (2008), Taniguchi (1974)]. Nanotechnology is distinct by its scale, one billionth ( $10^{-9}$ ) of a meter or the nanometer (nm). It is a form of molecular engineering, promises significant social benefits, including enhancements in health treatments and medical diagnosis, faster and cheaper materials, more efficient energy sources, and electronic products. The earliest, widespread description of nanotechnology referred to the particular technological goal of precisely manipulating atoms and molecules for the fabrication of macroscale products, also now referred to as molecular nanotechnology. A more generalized description of nanotechnology was subsequently established by the National Nanotechnology Initiative, which defined nanotechnology as the manipulation of matter with at least one dimension sized from 1 to 100 nm.

The manipulated materials by the use of the above technology are recognized as nanomaterials. Recently, the nanomaterials are receiving huge interest of the researchers engaged in the areas of environment, energy, catalysis, cosmetics, pesticides, stain resistant clothing, sunscreens, automotive paints, sporting goods and digital cameras, biomedical, electronics, health care, drug-gene delivery, mechanics, optics, chemical industries, space industries, science, light emitters, single electron transistors, nonlinear optical devices and photo-electrochemical applications.

These nanomaterials have attracted the researchers due to their minimal size, high surface area and enormous surface energy. These characteristics feature differentiated the nanomaterials with the bulk materials of the same composition concerning both physical and chemical properties like mechanical, thermal, biological, optical absorption, electrical conductivity and melting point. For instance, in nanomaterials, the optical properties such as refractive index and absorbance are directly related to the size and shape but the optical properties of the bulk material are fixed, regardless of its mass or volume. Therefore, the size and shape of the nanomaterials play a vital role in performing the novel application. On the basis of the core source material, the nanomaterials can be broadly categorized into (A) Metal oxide nanomaterials, (B), Metallic nanomaterials (C) Carbon-based nanomaterials.

Presently, metal oxide nanoparticles (MONPs) have fascinated much attention among the scientific community due to some unique features such as high surface energy, increased surface area to volume ratio, and durable surface absorption [Santos *et al.* (2016)]. Because of these properties, the MONPs are extensively used in many fields counting materials and engineering, chemistry, also in the medicinal area [Koch *et al.* (2007)]. They are iron oxide nanoparticles, titanium dioxide nanoparticles, cerium oxide nanoparticles, zinc oxide nanoparticles, etc. These can be synthesized through several methods such as chemical vapor deposition, laser ablation, photolithography, thermal decomposition, sol-gel process or hydrothermal reaction method and biological methods. Iron oxide nanoparticles have revealed its potential towards the biomedical applications such tissue repair, drug delivery, magnetic resonance imaging (MRI) and hyperthermia [Qiao *et al.* (2009), Gupta and Gupta (2005), Tong *et al.* (2017), Wei *et al.* (2017), Cano *et al.* (2017), Zhu *et al.* (2018), Laurent *et al.* (2008)]. Titanium oxide nanoparticles are used in water purification, printing ink,

cosmetics, medical implants, UV sunscreens, and sensors [Ou *et al.* (2017), Ramalingam *et al.* (2019), Abdolmazid *et al.* (2019), El-Naggar *et al.* (2016), Chen and Mao (2007), Pakrashi *et al.* (2014)]. Apart from this, titanium oxide nanoparticles are also used in the field of fuel cells, catalysis, photovoltaics, optoelectronics, smart windows, batteries, antifogging surfaces, and self-cleaning. Cerium oxide nanoparticles have shown mimetic properties of peroxidase, catalase oxidase, superoxide oxidase, and have materialized as an exciting material in severe biological fields, including bioanalysis, drug delivery, and biomedicine [Naganuma (2017), Charbgoon *et al.* (2017)]. Zinc oxide nanoparticles have been broadly used in the field of optoelectronics devices, laser technology and photocatalysis [Yang and Park (2007), Lu *et al.* (2015)]. Moreover, ZnO nanoparticles are also used in the ceramics industry because of their rigidity, hardness, and piezoelectric constant.

Metal nanoparticles (MNPs) have also been taken interesting research topics among the scientific community involved in nanoscience and nanotechnology at global scale. Recently, silver nanoparticles (AgNPs), gold nanoparticles (AuNPs), palladium (PdNPs), and platinum nanoparticles (PtNPs) are most widely used MNPs among them due to their broad range applicability in science and engineering. AgNPs are one of the noble metal nanoparticles because of their great interest due to their broad applicability in antiviral, antibacterial, and anticancer therapies [Saxena *et al.* (2012), Lu *et al.* (2008), Rahban *et al.* (2010)]. Besides this, AgNPs has also been used in biosensing, catalysis, wound dressings, medicine, water treatment, and surgical instruments [Dahl *et al.* (2007), Dubas and Pimpan (2008), Filippo *et al.* (2010), Vivek *et al.* (2012), Kumar-Krishnan *et al.* (2016)]. AuNPs have also played a significant role in the several areas counting catalysis, biosensing, anticancer, medicine, electronics etc. [Varun *et al.* (2017), Shen *et al.* (2017), Ramachandran

*et al.* (2017), Ribeiro *et al.* (2017), Daniel and Astruc (2004), Farooq *et al.* (2018) Mobed *et al.* (2020)]. The PtNPs are used in fuel cells and hydrogen storage materials. PtNPs acts as a significant catalyst than bulk materials [Schmidt *et al.* (1999), Bendale *et al.* (2017), Thirumurugan *et al.* (2016), Tahir *et al.* (2017), Cheng *et al.* (2009)]. Several platinum-based complexes are being used against both gram-positive and gram-negative bacteria as a potent antibacterial agent [Sharma (2017)]. The PdNPs show exceptional catalytic activity and have been used extensively as a catalyst in the field of catalysis [Favier *et al.* (2019), Arsiya *et al.* (2017), Li *et al.* 2017)]. In addition to this, PdNPs are also used in different applications such as carbon-carbon coupling reaction, oxidation, hydrogenation, and electrochemical reactions in hydrogen storage, fuel cell, and gas sensing [Ismail *et al.* (2017), Kumar *et al.* (2018), Yang *et al.* (2019), Albani *et al.* (2016)].

Now a day, the carbon-based nanomaterials like, fullerene, Carbon Nanotubes (CNTs), Graphene, graphite, and graphene oxide have revealed greater potential in various applications such as biosensing, electronics, optics, and biomedicine. Currently, carbon based materials exhibit utterly different properties due to the existence of various allotropes as well as different nanostructures such as diamond, graphite, graphene oxide, graphene, fullerene, and carbon nanotubes (CNTs), as shown in **Figure 1.1** [Mauter *et al.* (2010), Scida *et al.* (2011)]. Due to the many advantageous properties such as excellent resistance to corrosion, high mechanical strength, and attractive optical properties, they could be used in the severe field which includes energy storage, biology, and medicine [Atchudan *et al.* (2015)].

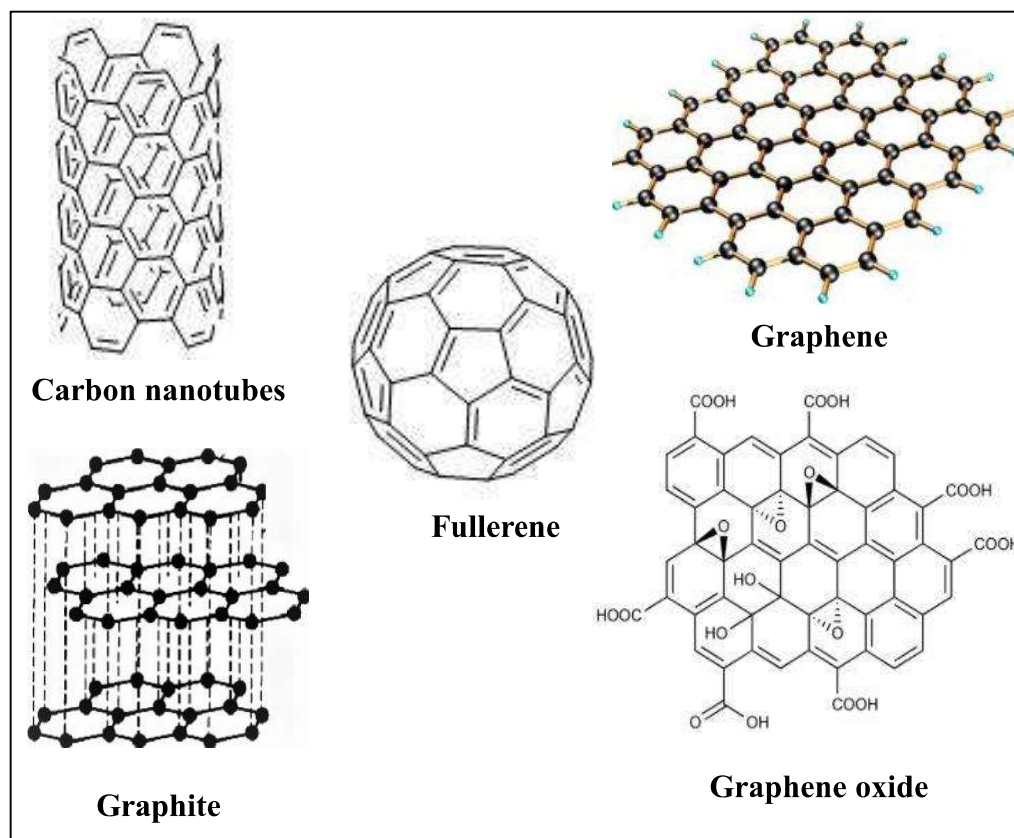


**Figure 1.1 Structure of various allotropes and nanostructure of carbon.**

## 1.2. Carbon quantum dots

During the last decades, metal based semiconductor quantum dots (QDs) have been investigated for their resilient and tunable fluorescence emission properties, which enable their applications in biosensing and bioimaging. However, they hold certain prohibition toward their applicability in the biomedical field or several other analytical applications as they contain heavy metal core which is not environmentally compatible [Larson *et al.* (2003), Cao *et al.* (2007), Liu *et al.* (2009), Tan *et al.* (2015)]. Heavy metals are highly toxic even at very low concentrations, thus restricted the applicability in clinical analysis [Geys *et al.* (2008), Lin *et al.* (2008)]. Carbon quantum dots (CQDs) turned into a new class of

carbonaceous materials in a carbon family and has become a mounting star among the scientific community over the past decades [Demchenko *et al.* (2013), Zheng *et al.* (2015), Sinduja *et al.* (2015)]. It has been categorized into a 0D materials. Xu's Group have first discovered these materials in 2004 during the electrophoresis of single-walled carbon nanotubes (SWCNTs) from arc-discharged soot, accidentally [Xu *et al.* (2004)]. Thus, due to their interesting features such as low cyto-toxicity, ease of synthesis, facile surface functionalization, sturdy photo-stability, high photo-response, tunable excitation-emission and catalysis properties, it could be broadly used in the application of bio-imaging, drug delivery, optronic devices, sensor and catalyst [Chen *et al.* (2010), Ajayan and Zhou (2001), Pardo *et al.* (2018), Taghavi *et al.* (2020), Baptista *et al.* (2015), Cayuela *et al.* (2016)].

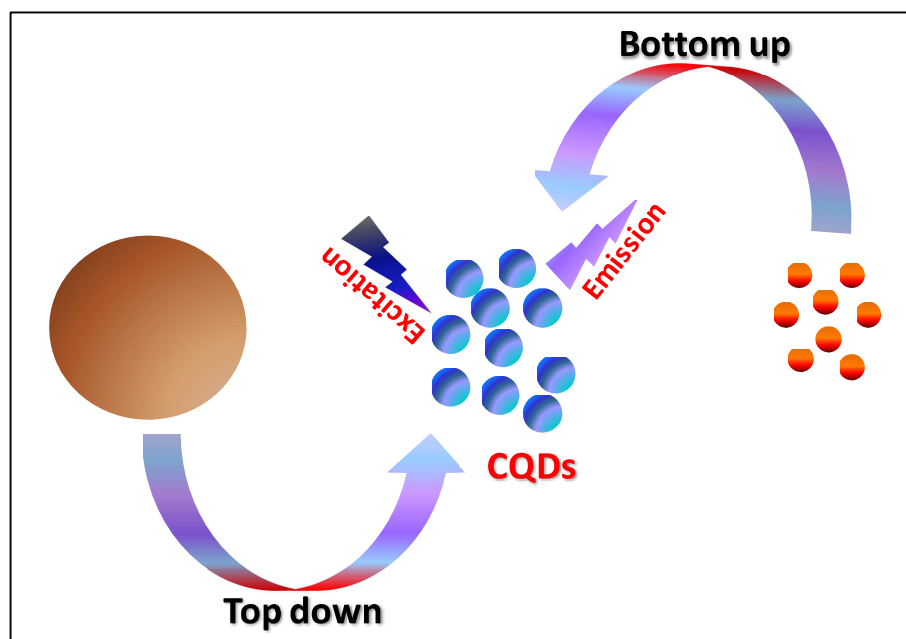
CQDs are generally spherical and quasi-spherical nanoparticles in shape where core contains largely  $sp^2$  and  $sp^3$  hybridized carbon and outer surface grasps substantial amount of functional group specifically carboxylic, hydroxyl, carbonyl, amine and many more depending on the precursors [Yang *et al.* (2009), Baker and Baker (2010)]. These surface functional groups made them soluble in an aqueous medium. They have size ranges between 1 and 10 nm [Zhou *et al.* (2017), Zuo *et al.* (2016)]. CQDs have poor crystallinity as they exhibit peak broadening at around  $2\theta$  and produces more surface defect compare to graphite. The defect on the surface can be created through the various functionalization and doping which may serve as photoexciton electron capture, therefore leading to surface related fluorescence properties.

There are many organic compounds, such as ascorbic acid, tartaric acid, citric acid, glycol, glucose, sucrose, and glycerol that have been used for the synthesis of CQDs. For surface passivation, many organic polymeric moieties such as polyethyleneimine,

polyethylene glycol, and 4,7,10-trioxa-1,13-tridecanediamine, etc. have been frequently used [Alam *et al.* (2015), Bano *et al.* (2018)]. At present, the CQDs are being synthesized via natural organic precursors. To date, numerous studies have utilized natural green sources counting pomelo peel, soybean, orange juice, milk, potato, plant leaves, soy milk, cocoon silk, etc. for the synthesis of CQDs have been reported [Li *et al.* (2013), Sahu *et al.* (2012), Lu *et al.* (2013), Zhu *et al.* (2012), Lu *et al.* (2017), Lu *et al.* (2012), Li *et al.* (2013)]. Though, the key challenge is still to develop CQDs with high fluorescence quantum yields (QY).

### 1.2.1. Synthesis of CQDs

Along the direction of size development of the selected organic materials, the fabrication of CQDs can generally be grouped into two kinds of approaches (i) Top-down (ii) Bottom-up (Scheme 1.1).



**Scheme 1.1** An illustration of techniques for the synthesis of fluorescence CQDs.

### 1.2.1.1. Top down approach

In this methodology, CQDs are synthesized through the exfoliating small carbon nanoparticles from the larger organic precursors such as carbon nanotubes, carbon soot, carbon rods, carbon fibers, single walled carbon nanotubes, fullerene, graphite, graphene oxide, etc., by using various techniques which include the method of arc discharge, laser ablation, and electrochemical oxidation [Sun *et al.* (2006), Zheng *et al.* (2009), Li *et al.* (2010)].

#### A. Arc Discharge

The synthesis of fluorescent CQDs was first reported through the use of the Arc discharge method. It was the accidental discovery of CQDs during the purification of single walled carbon nanotubes (SWCNTs). In this study, Xu's group isolated a mixture of fluorescent carbon through the electrophoretic method from the crude SWCNTs soot. The measured fluorescent QY was 1.66 % at 366 nm exciton wavelength [Xu *et al.* (2004)]. Production of CQDs from this method possesses some advantages such as evolvment of the simple purification process, the use of eco-friendly techniques, the formation of small size nanoparticles, and its ability to exhibit different fluorescent colors without any surface modification. Though, low fluorescent yield, development of complex mixtures, and difficulty in post surface modification are the major shortcoming of this method.

#### B. Electrochemical oxidation

The production of CQDs through the electrochemical oxidation of MWCNTs and graphite has attained more attention because of its easy-synthesis process, easy manipulation, economical, and high productivity. This method was first reported by

Zhou's group [Zhou *et al.* (2007)]. They proposed the synthesis of carbon nanocrystals through electrochemical route in a degassed acetonitrile solution in the attendance of supporting electrolyte tetrabutylammonium perchlorate. They developed MWCNT-based carbon paper which was selected as a working electrode and was coupled with an Ag/AgClO<sub>4</sub> reference electrode and with a Pt wire counter electrode for conducting the electrochemical synthesis. Blue luminescent CDs were obtained along with QY 6.4% by precisely controlling the cycling voltage. Subsequently, Zheng *et al.* also reported the synthesis of CNCs electrochemically from the graphite as a supporting electrode [Zheng *et al.* (2009)]. Ag/AgCl reference electrode, and a Pt mesh counter electrode at pH 7 in phosphate buffer solution. Zhao *et al.* also synthesized fluorescent CNCs in aqueous solution through the electrochemical oxidation of graphite by using the graphite rod as working electrode [Zhao *et al.* (2008)]. Apart from this, several research groups also reported the synthesis of CQDs by the technique of the electrochemical route. However, the use of post surface functionalization/passivation for obtaining higher QY made this route more time-consuming, complex, and economical.

### **C. Laser Ablation**

Sun's group in 2006 was reported this method, firstly which holds the irradiation of laser beam on precursor molecule leading to the synthesis of CQDs [Sun *et al.* (2006)]. The used laser in this method was Q-switched Nd: YAG laser (1064 nm, 10 Hz). The obtained CQDs from this synthesis method was typically non-fluorescent in nature, therefore post surface modification was required which increased QY upto

10%. Thus, the result suggests that the CQDs formed through this method suffer the use of several complex steps to show proficient photoluminescence.

The obtained CQDs through the top-down method possess perfect  $sp^2$  structure but the lack of bright photoluminescent properties. However; by the use of some chemical modification luminescent properties of CQDs could be enhanced. Though, this method is beneficial and expedient for the microsystem industries. Still, this approach has some drawbacks in obtaining pure nanomaterials from the bulky precursor and employed an expensive purification process.

#### **1.2.1.2. Bottom-up approach**

This method is more comfortable to implement for the large scale production of treatment, microwave-assisted irradiation, ultrasonic-assisted methods, hydrothermal or solvothermal treatment [Liu *et al.* (2007), Wang *et al.* (2015)].

##### **A. Plasma treatment**

Jiang *et al.* demonstrated the development of uniform CQDs by using a new generation all-in-one small submerged-arc plasma reactor that benefited from the helium plasma-generated free radicals [Jiang *et al.* (2010)]. This process combined their synthesis and functionalization together. Nevertheless, due to the requirement of a special set-up, no further additional studies were then reported.

##### **B. Microwave-assisted irradiation**

Microwave irradiation is a speedy and economical method to produce CQDs with sturdy fluorescent properties. It is a suitable method compare to others as it requires very little to carbonize the small organic precursors through microwave heating. The

size and optical properties of CQDs could be tuned by the reaction time. Zhu *et al.* reported a simple microwave pyrolysis approach to synthesize fluorescent CQDs. In this study, CQDs were synthesized by heating of poly (ethylene glycol) (PEG-200) and saccharide for 2-10 mins under the microwave (500W) [Zhu *et al.* (2009)]. However, the challenging separation process, purification step and non-uniform particle size restrict their potential application.

### **C. Ultrasonic-assisted Methods**

It is approved that ultrasound can generate alternant high pressure and low pressure waves in aqueous solution owing to the synthesis and collapse of small vacuum bubbles. These cavitations cause high-speed impinging liquid jets, strong hydrodynamic shear forces and deagglomeration [Li *et al.* (2012); Park *et al.* (2014); Li *et al.* (2011), Zhuo *et al.* (2012)]. Therefore, the energy produced by the ultrasonic waves can cleave the larger organic precursors and produces nanorange CQDs. In another literature, Li *et al.* described a greener route for producing water soluble CQDs via ultrasonic treatment active carbon in H<sub>2</sub>O<sub>2</sub> solution [Li *et al.* (2011)]. The as-synthesized CQDs were exhibited sturdy visible emission properties along with excellent optical properties.

### **D. Hydrothermal and solvothermal carbonization**

Hydrothermal carbonization is one of the most reported routes for the synthesis of CQDs. In this technique an aqueous solution of chosen organic precursors, such as polyols, amino acids, glucose [Wang *et al.* (2015)], proteins, polymers, some wastes and natural products are sealed in a Teflon lined reactor and then implemented to react for hours at high temperature and pressure. Wei's group synthesized nitrogen-

doped CQDs by the hydrothermal treatment of shrimp waste as a starting reactant [Wei *et al.* (2015)]. In another study, Zhao's synthesized nitrogen and sulfur co-doped CQDs through the hydrothermal treatment by using garlic cloves as a starting material at temperature 200 °C for four hours [Zhao *et al.* (2015)]. Fascinatingly, Briscoe's group synthesized different CQDs from ethanolic solutions of glucose, chitin, and chitosan [Briscoe *et al.* (2015)]. In this synthesis process, the reaction solution suffered hydrothermal treatment for the time period of six hours at 200 °C. In a recent years, the CQDs obtained by this method has some advantages over others in aspects of low cost, ease of operation, controllability, easy feasibility, low labor costs, and environmental friendliness. Apart from this, the CQDs from this method synthesize in a closed vessels, which prevent the volatilization of toxic and harmful chemicals. The solvothermal method is analogous to the hydrothermal with the significant modification in a solvent used. In this process, the organic solvent is used instead of water. The used solvent in this process is ammonia, hydrogen peroxide, dimethylformamide, alcohol and other inorganic and organic solvents.

## **1.2.2. Optical properties of CQDs**

### **1.2.2.1. Absorption**

CQDs generally exhibit absorption peak in between 280 nm and 350 nm along with a tail extending in the visible region. The shoulder peaks at 280 nm correspond to a  $\pi-\pi^*$  transition of the aromatic C=C bond and 350 nm corresponds to an  $n-\pi^*$  transition of the C=O bond, as earlier reported [Hu *et al.* (2014)]. The tail in the visible region might be credited to the surface associated chemical groups. The attached surface group can adjust the

absorbance position, leads to the colorful CQDs and made them as a probe for detecting colorimetrically.

### 1.2.2.2. Fluorescence

Fluorescence emission of CQDs generally follows the Stokes type emission, where the emission wavelength is greater than the exciton wavelength. It is the exciting and most intriguing feature of CQDs and has been employed in the several areas of research including sensing and other analytical applications. At present, there have been various reported literatures on the origin of fluorescence emissions in CQDs [Gokus *et al.* (2009); Demchenko *et al.* (2013), Baker *et al.* (2010)]. Though; the exact mechanism is still arguable amongst the researcher community and became a challenging task. A closer inspection advocates that most of the observed fluorescence emissions could be categorized into two categories. The first one is the bandgap transitions arise from the conjugated  $\pi$ -domains, and the other one with more complex origins that are corresponded with the defects in the carbon skeleton.

Some literature related the fluorescence of CQDs with their excitation wavelength ( $\lambda_{\text{ex}}$ ) properties. Sun *et al.* reported that fluorescent CQDs modified with polyethylene glycol (PEG 1500N) or propionylethyleneimine-co-ethyleneimine (PPEI-EI) display obvious  $\lambda_{\text{ex}}$ -dependent emission [Sun *et al.* (2006)]. This result is further confirmed by the Li's group in 2018 [Li *et al.* (2018)]. Furthermore, Mohapatra's group clearly confirmed the excitation dependent properties of CQDs with increasing size on comparing with larger carbon nanoparticles when both were excited at 390 nm. Eventually, the band gap from the quantum confinement effect and presence of  $sp^2$  hybridized sites would vary along with different sizes of CQDs. They have also reported, that different fluorescence emission on different

excitation wavelengths may be due to the different emissive trapped state, excitons of carbon, free zig-zag sites and aromatic conjugated structures.

Some people have reported that fluorescence of CQDs is originated from the defects on their surface [Ming *et al.* (2012)]. The defect sites refer to the disordered  $sp^2$  domain which leads to the surface energy traps. Thus, the  $sp^2$  and  $sp^3$  hybridized carbon atoms, as well as functionalized surface defects, can result in the fluorescence emission of CQDs. Furthermore, if CQDs are functionalized or surface passivated, it will result in more stabilization of the surface defects which in turn leads to facilitate radiative recombination of the electron-hole pairs, confined on the surface.

### 1.2.2.3. Phosphorescence

The phosphorescence properties in CQDs were also originated. A pure organic room temperature phosphorescent (RTP) water soluble material was obtained along with phosphorescent lifetime up to the 380 ms [Deng *et al.* (2013)]. At room temperature, phosphorescence in CQDs could be observed under UV light of 325 nm exciton by dispersing the CQDs into a polyvinyl alcohol (PVA) matrix. It was also suggested that the phosphorescence originated from the triplet excited states of aromatic carbonyls on the surface of CQDs [Bolto *et al.* (2011), Wardle (2009)]. Hydrogen bonding is usually important for RTP because they could effectively lock the emissive species and inhibit their intramolecular motions, the non-radiative relaxation channel.

### **1.2.3. The effect of doping elements on the fluorescence properties of CQDs**

Most of the CQDs have relatively low quantum yield even after surface functionalization and passivation compared to the conventional semiconductor quantum dots. Thus; improving the fluorescent properties of CQDs is a challenging task and highly required to expand their biological and other analytical application. Doping is one of the important factors to enhance the optronic properties of CQDs. Currently, the doping approach has been considered as the most promising production pathway to yield highly fluorescent CQDs by tuning the fluorescent properties. As reported earlier, doping could be obtained by both metal atoms as well as nonmetal atoms/heteroatom. Metal doping is a useful tool to enlarge the fluorescence quantum yield of CQDs but the main obstacle of this method is the increased toxicity related to health and the environment. Thus; heteroatom doping has been proven as an alternative method for enhancing the optical and electronic properties of CQDs. Plenty of single atom doping and co-doping have been reported to explore the fluorescence properties of CQDs as described.

#### **1.2.3.1. Single-heteroatoms doping**

##### **A. N-Doped CQDs**

Nitrogen is the widely used hetero element to increase the fluorescence properties of CQDs. Due to the similar size of C and N, nitrogen doped CQDs could be obtained. Nitrogen changes the internal electronic structure of CQDs by injecting electron, which effectively enhances their luminescent properties. N-doped CQDs exhibit outstanding properties in various analytical approaches and biological applications. Various method have already been reported for the CQDs synthesis. One of the main approaches emphasizes on leveraging the richness and sustainability of natural

biomass precursors to offer an economical and greener route for producing high yield fluorescent CQDs. Sun's group reported the highly luminescent nitrogen-doped CQDs from the hydrothermal treatment of grass. In this study, they heated grass at 180 °C for 3 hours and afterward centrifuged to acquire pure CQDs. This research work also emphasizes the temperature dependent variation on the fluorescence QY of CQDs, which was in the range between 2.5 and 6% amid the temperature range 150–200 °C [Liu *et al.* (2012)]. Wu *et al.* reported a one-pot hydrothermal synthesis of CQDs from the bombyxmorisilk at 190 °C for 3 hours in NaOH solution holding nitrogen up to 18.36–18.65%. The resultant fluorescence quantum yield of N-doped CQDs was 13.9 % [Wu *et al.* (2013)]. In another research, Zhu *et al.* synthesized a highly luminescent N-doped CQDs from the hydrothermal treatment of soymilk. The fluorescence QY was measured to be 2.6 % at N-content of 10.39 wt% [Zhu *et al.* (2012)]. In a study, Dey *et al.* synthesized CQDs with blue emission through the reaction of glucose and urea by the method of hydrothermal and microwave irradiation; however the resultant QY were 0.7% and 1%, respectively [Dey *et al.* (2014)]. Subsequently, Ding *et al.* were also reported N-doped CQDs through the novel precursor (PVP) and trioxa-1,13-tridecanediamine (TTDDA)-passivated CQDs. The synthesized CQDs exhibited multicolor emission with relatively high QY of 19.6% [Ding *et al.* (2014)]. Later, Wu *et al.* were fabricated N-doped CQDs with improved QY of 51% through the hydrothermal method (11 h at 230 °C) by using ethylenediamine as N dopant, and a non-toxic carbon precursor microcrystalline cellulose consisted 1,4-anhydro-D-glucopyranose units [Wu *et al.* (2017)].

### **B. S-Doped CQDs**

In a comparison of the extent of research for producing N-doped CQDs, S atom doped CQDs has been rarely stated. Currently, S-doped CQDs have held great attention because of fascinating optical properties. The S-doped CQDs could be achieved by the different S containing precursors such as sulfuric acid, hydrogen sulfide, and so on. Chandra *et al.* synthesized S-doped CQDs from the thiomalic acid (TMA) as the carbonaceous material where TMA was pyrolyzed in sulfuric acid for four hours at 90 °C and products were obtained by solvent extractions [Chandra *et al.* (2013)]. In a recent study, Travlou *et al.* were designed two types of S-doped CQDs through the hydrothermal treatment of two different precursors poly(sodium 4-styrene sulfonate) and poly(4-styrene sulfonic acid co-maleic acid) with improved QY of 9% and 6%, respectively [Travlou *et al.* (2017)].

### **C. B-Doped CQDs**

B-doped CQDs are also observed as boron is the left neighbor of carbon in a periodic table. Feng *et al.* synthesized B-Doped CQDs by using hydroquinone as the carbon and BBr<sub>3</sub> as a boron precursors. The as-synthesized B-doped CDs had a size distribution of 8 to 22 nm. It displayed a blue color fluorescence emission under UV-light along with QY up to 14.8% [Shan *et al.* (2014)]. This outcome suggested that boron can be used in the doping of CQDs and act as an active site for charge transfer in CQDs. In addition, Lu *et al.* also reported a B-doped CDs through the hydrothermal approach with distinctive solid-state fluorescence. The resultant CDs had high fluorescence QY up to 22% [Shen *et al.* (2015)].

#### **D. P-Doped CQDs**

Recently, numerous research groups fruitfully reported P-doped CQDs from the different phosphorus holding precursors as its capability to act as an n-type donor, could form substitutional defects in CQDs. Feng's group employed P-doped CQDs by using hydroquinone as a carbon precursor and  $\text{PBr}_3$  as a phosphorous dopant [Zhou *et al.* (2014)]. The synthesized P-doped CQDs had a broad size distribution in between 5 and 15 nm whereas fluorescence QY was 25% at 372 nm excitation wavelength. Lately, Wang *et al.* synthesized green emitted fluorescent P-doped CQDs with enhanced QY of 21.65% through the microwave reaction (700 W for 10 min) amid ethylenediamine and phytic acid (P precursors) [Wang *et al.* (2013)]. In a recent investigation, Yang *et al.* were produced P-doped CQDs along with high QY 3.5% through the hydrothermal treatment of phytic acid and sodium citrate [Yang *et al.* (2018)]. In this study, phytic acid is used as a P dopant which consisted rigid C-P bonds, abundant phosphate group and completely natural.

In summary, single-atom doping can efficiently passivate the surface active sites by stabilization of the excitons in the CQDs which leads to improve the emission properties. The percentage of doped atoms in CQDs plays an essential role in generating high fluorescence QY. Higher the content of heteroatoms in a synthesized CQDs, more surface states get formed on doped CDs which traps more electrons, resulting in a high fluorescence QY.

#### **1.2.3.2. Co-doping with multi heteroatoms**

Co-doping multi heteroatoms is also a significant tool for enhancing fluorescence QY because it can create a distinctive electronic structure owing to the co-operative effect or

synergistic effect amid the doped heteroatoms in CQDs. This section describes the importance of co-doping in CQDs on fluorescence QY.

#### **A. N and S co-doped CQDs**

Co-doping with N and S has been found as an ideal pathway for enhancing the fluorescence QY of CQDs. Apart from this co-doping also delivers more active sites in CQDs to widen their potential application in nanomedicine, biosensing, and photocatalysis. N and S doped CQDs has been investigated by a various researcher community. Dong *et al.* first designed N, S doped CQDs via the hydrothermal treatment of L-Cysteine and citric acid [Dong *et al.* (2013)]. In this synthesis process citric acid was used as a carbonaceous material and L-cysteine was used for the N and S precursors. The synthesized CQDs showed excitation dependent behavior along with fluorescence QY of 73%. Following a similar approach, Xue *et al.* were synthesized S, N-doped CQDs along with high fluorescence QY 74.15% by using ammonium thiocyanate as N and S precursors [Xue *et al.* (2016)]. In another study, N and S doped CQDs were successfully obtained with high fluorescence QY 73.1 % via the use of thiourea as N and S precursors [Wang *et al.* (2016)]. Besides, Ding *et al.* were also produced N and S doped CQDs via the hydrothermal treatment of  $\alpha$ -lipoic acid. The synthesized CQDs from this method had relatively high fluorescence QY up to 54.4% with an average particle size distribution 2.7 nm [Ding *et al.* (2014)].

#### **B. N and P co-doped CQDs**

N and P doped CQDs are expected to obtain due to combined effects from the doped atoms. Sahu and co-workers reported the first strategy to produce N and P doped CQDs through the hydrothermal process. They synthesized N and P doped CQDs

with high fluorescence QY by using citric acid and  $(\text{NH}_4)_2\text{HPO}_4$ . The resultant N and P doped CQDs had a high fluorescence QY up to 59% [Chandra *et al.* (2016)]. Similar literature was also reported by Zhang and co-workers and the resultant CQDs exhibited excitation dependent emission and had a relatively high fluorescence QY 23.5% under the excitation of 340 nm [Gong *et al.* (2016)]. Therefore, doping with N and P in a carbonaceous core improves the optronic properties of CQDs and found to be a promising candidate towards the increase in fluorescence QY.

### **C. N and B co-doped CQDs**

N and B doped CQDs have also been observed as nitrogen is a right neighbor of carbon and boron is left neighbor of carbon. Co-doping with N and B in a CQDs is of fundamental as well as practical prominence. Liu *et al.* synthesized blue emitting B and N doped CQDs via the hydrothermal treatment of Branched polyethylenimine and 4-formylboronic acid for 8 h at 220 °C, which had fluorescence QY 15.85% [Liu *et al.* (2017)]. Also, Guo *et al.* fabricated B and N doped CQDs through the hydrothermal treatment of 2-hydroxyphenylboronic acid and ethylenediamine precursors for 12 h at 180 °C. In this study, the prepared N,B-doped CQDs exhibited yellow-green emission which had fluorescence QY of 6.59% [Guo *et al.* (2017)].

### **D. B and S co-doped CQDs**

In a literature, B and S co-doped CQDs has also been observed. Zhao *et al.* have prepared B and S co-doped CQDs by the hydrothermal treatment of poly (sodium-p-styrene sulfonate) and borax as the major B and S precursors [Liu *et al.* (2017)]. The synthesized CQDs had relatively high QY up to 25.7%, along with blue emission. The synthesized CQDs exhibited excitation dependent emission along with a large

blue shift in emission, which was credited to the strong electron-withdrawing ability of boron.

Therefore, co-doped CQDs have also originated to attract more devotion because of their excellent fluorescence. However, the exact mechanisms still remain uncertain, it is believed that the co-doping technique extends the applications of CQDs in photocatalysis, chemical sensing, biosensing, and nanomedicine.

### 1.3. Fluorescence quantum yield

It is defined as the ratio of the number of the photon emitted to the number of photons absorbed, as shown in **equation 1.1**. Since all photon absorbed does not lead to the formation of the product; therefore, the typical value of QY will be less than one.

$$\text{Quantum yield (QY)} = \frac{\text{Photon emitted}}{\text{Photon absorbed}} \quad 1.1$$

The quantum yield of the fluorophore materials is determined relative to the quantum yield of the standard fluorophore materials.

### 1.4. Basic principle of Fluorescence quenching

The most of the CQDs which have been used in the sensing was based on the quenching. Quenching is generally decreased in the emission of fluorophore molecule in the presence of other species or analyte in the solution. There are some sensing principles based on the fluorescence quenching of CQDs.

### 1.4.1. Static quenching

Static quenching arises when a nonfluorescent ground-state complex is formed over the interaction between CQDs and absorber or quencher molecules. The complex immediately returns to the ground state without emission of a photon when the complex absorbs light. For static quenching (a)  $\tau_0/\tau=1$ ; (b) the formation of the ground-state complex can result in the change of the absorption spectrum of the CQDs.

In such a case, the dependence of fluorescence with the concentration of quencher follow the following **equation 1.2**.

$$F_0/F = 1+K_{sv} [Q] \quad 1.2$$

where “F” is the fluorescence intensity of the sensor in the presence of analyte and “F<sub>0</sub>” is the fluorescence intensity of the sensor. “K<sub>sv</sub>” is the Stern-Volmer quenching constant and “[Q]” is the concentration of quencher.

### 1.4.2. Dynamic quenching

Dynamic quenching is also known as collisional quenching, in which the fluorescence intensity of fluorophore decrease by excited state quencher- fluorophore interaction. The fluorescence lifetime of fluorophore decrease in the presence of quencher molecules whereas on increasing the temperature the Stern-Volmer constant (K<sub>sv</sub>) increase due to the increase in the diffusion rate.

### 1.4.3. Inner filter effect

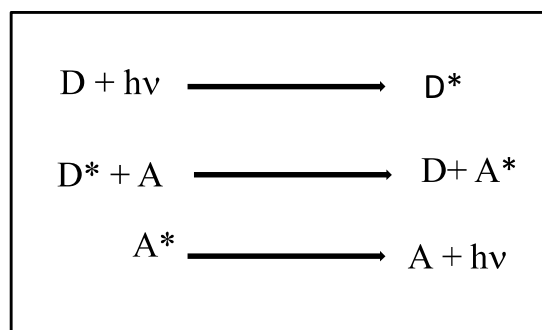
The inner filter effect (IFE) was formerly measured as a source of inaccuracy in fluorescence analysis. It requires an excellent spectral overlap amid the absorption band of the absorber and the excitation band and/or emission band of the fluorophore. Recently, it has

become as an important non-irradiation energy conversion in a spectroscopic techniques as it provides apparent advantages of expediency, flexibility, simplicity, straightforwardness, and rapidity in the chemical sensing, biosensing, industries, and future other analytical and environmental applications [Yuan *et al.* (1987), Gabor & Walt (1981), He *et al.* (1993)].

IFE based sensing system requires two optical units i.e., acceptor/quencher and fluorophore. For the excellent IFE activity, the following facts should be followed (1) The absorption spectrum of quencher or acceptor must hold an adequate overlap with the excitation and/or emission spectrum of the fluorophore, thus the fluorescence emission of fluorophore molecule could be adjusted by the use of quencher molecule. The efficacy of IFE is dependent on the extent of spectral overlap. Consequently, for the IFE-based fluorescent assay, it is necessary to choose a better absorber-fluorophore pair. (2) The fluorescence and absorption features of the selected fluorophore and absorber should be free from the effect of external factors. Hence, for the designing an IFE-based sensing assay, it has to choose an analyte-sensitive absorber, and the excitation/emission intensity of fluorophore [Yang *et al.* (2000), Shao *et al.* (2005), Lakowicz (2013)].

#### **1.4.4. Fluorescence resonance energy transfer (FRET)**

It is a distance dependent radiationless phenomenon from an excited fluorophore molecule to the quencher or acceptor molecule within some distance. It is different from static and dynamic quenching. In the FRET process, firstly donor fluorophore molecule absorbs the energy of excitation wavelength and transfer the excitation energy to the acceptor one, as shown in **equation 1.3** [Dong *et al.* (2010), Wu *et al.* (2017), Oh *et al.* (2005)].



1.3

The energy transfer demonstrates itself through a decrease of the donor fluorescence and a reduction of excited state lifetime accompanied also by an increase in acceptor fluorescence intensity. **Figure 1.2** demonstrates a Jablonski diagram which explains the transitions involved amid the emission of donor and absorbance of acceptor during the FRET process. In the presence of a suitable quencher or acceptor, a fluorophore molecule can transfer its excited state energy directly to the acceptor without emitting a photon [Kozlov *et al.* (1997)].

For the FRET process to occur, few conditions must be satisfied which are: (i) the spectral overlap must occur amid the fluorescence emission or excitation spectrum of fluorophore molecule and absorption of the acceptor molecule (ii) The lifetime of the fluorophore molecule must have sufficient duration of time to allow the FRET. In summary, the rate of FRET is governed by the degree of spectral overlap among the donor and acceptor molecules [Selvin (2000), Heyduk (2002), Hink *et al.* (2002), Parsons *et al.* (2004), Lakowicz (2013)].

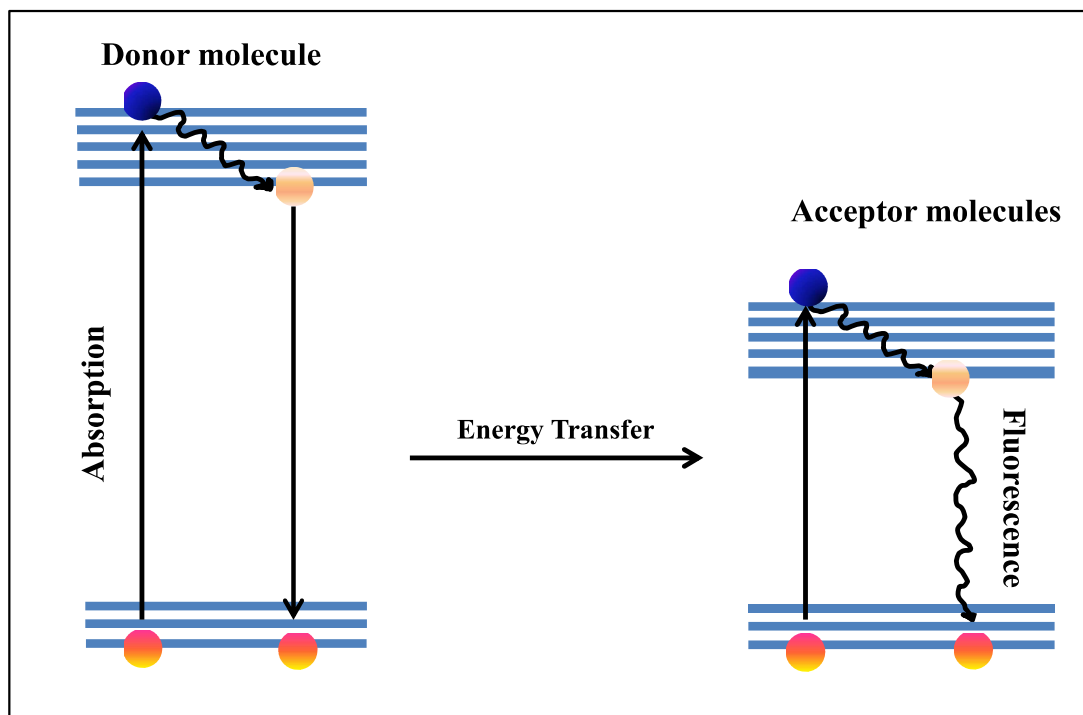


Figure 1.2 Illustration of the FRET process through the Jablonski diagram

## 1.5. Applications

### 1.5.1. Light emitting Diodes (LED's)

To fabricate the light emitting devices, a film of CQDs are embedded on the polymer, and the polymer matrix provides mechanical support as well as prevent the solid state quenching of CQDs. The resulting films was cost effective, highly flexible, ecofriendly, thermally stable, mechanically robust and potentially utilize for solid state lighting system [Mao *et al.* (2014)]. In recent years, many researchers have opened up the usage of doped and un-doped CQDs in a LED sources. Recently, Khan *et al.* have developed an LED by packing a flexible film on the top of a UV-Chip (395 nm), based on N-doped CQDs and

polyvinyl alcohol (PVA) composite which have provided a potentially vigorous green light. In this study green emissive CQDs were prepared by using urea and ammonium citrate as a precursors via solid state reaction and subsequently emerged into a PVA matrix [Khan *et al.* 2018)]. Zhou *et al.* have designed white LED by merging (a) robust yellow emitting fluorescent material by congregation of as-prepared N and S co-doped CQDs and epoxyresin, (b) blue chip at 465 nm [Zhou *et al.* (2017)]. In this study, it has been exposed that CIE (Commission Internationale de l'Éclairage) coordinates of as-prepared white LED (0.27, 0.29), which was near to the pure white light coordinate (0.33, 0.33).

### 1.5.2. Solar cells

Solar cells are extensively used in the fabrication of electricity for rising global demand for energy, and utilized as an alternative to the conventional sources, such as coal. Recently, doped or co-doped CQDs have been consumed in the conversion of solar energy into electrical energy by using solar cells because of their sturdy photostability. Zhang *et al.* have reported the N-doped CQDs as metal-free sensitizers in dye-sensitized solar cells (DSSCs) [Zhang *et al.* (2013)]. In this literature, CQDs-sensitized titanium oxide (TiO<sub>2</sub>) electrodes were prepared through the hydrothermal treatment for 4 h at 100 °C between TiO<sub>2</sub> and N-doped CQDs. By using a similar approach, Wang *et al.* have designed solar cells (DSSC) by sandwiching gel electrolytes between a platinum (Pt) counter electrode and TiO<sub>2</sub> electrode sensitized N-doped CQDs [Wang *et al.* (2016)].

### 1.5.3. Fluorescent ink

It is found that CQDs can also be used in the fluorescent ink. In a study, Guo *et al.* were fabricated B and N-doped CQDs, which could be utilized as a fluorescent ink in writing a letters/numbers/characters [Guo *et al.* (2017)]. In this study, it was found that with the

decreased concentration of CQDs color of letters/numbers/characters changes from light yellow to colorless under the visible light. Moreover, they exhibited blue color under 365 nm UV-excitation wavelength, which showed the three month fluorescence stability, exploring their potential applicability for invisible fluorescent ink for anti-counterfeiting. By using a similar approach, Bandi *et al.* have also discovered the potential applicability of N and S co-doped CQDs for fluorescent ink for use in anti-counterfeiting [Bandi *et al.* (2018)].

#### 1.5.4. Drug delivery

Recently, nanoparticles expand more devotion to the drug delivery system. CQDs serve as a good alternative among other nanoparticles because of the rapidly and economical synthesis process, high surface area, enormous surface energy, and ease of functionalization deliver an outstanding platform for conjugation of drugs molecule according to the targeting agent and expanding the drugs choice for delivery. Furthermore, the nontoxicity and biocompatibility of CQDs favored their use as drugs vehicle in a biological system. The anticancer agents (drugs) were conjugated over the surface of CQDs and *in vivo* drugs distribution were monitored by the fluorescence signal of CQDs. Pandey *et al.* were used CQDs functionalized gold nanorods for the delivery of doxorubicin [Pandey *et al.* (2013)]. In an investigation, Kim *et al.* coupled the CQDs with gold nanoparticle and conjugated the PEI-pDNA on the surface of assembled CQDs-gold nanoparticle for delivering DNA into the cells [Kim *et al.* (2013)]. Additionally, a broad spectrum antibiotic, ciprofloxacin attached to CQDs, which offers a proficient nanocarrier for controlled release of drugs under physiological conditions [Thakur *et al.* (2014)]. Subsequently, Zheng *et al.* synthesized the multifunctional theranostic agent by adhering the oxidized oxaliplatin onto the surface of

CDs (CD-Oxa) and demonstrated that CD-Oxa possesses good bioimaging and anticancer effects [Zheng *et al.* (2014)].

### 1.5.5. Cellular imaging

On comparing with traditional organic and inorganic fluorescent molecules, CQDs are more capable candidates for bioimaging owing to their unique combination of resistance to photobleaching, low toxicity, excellent water solubility, and intense luminescence with high fluorescence QY. In an investigation, Sun *et al.* conveyed the use of CQDs for cell imaging applications *in vivo* as well as *in vitro* [Sun *et al.* (2006)]. Yang *et al.* proposed the applicability of CQDs in a fluorescence contrast agent in mice by multimodal imaging technology, which comprises the magnetic resonance imaging (MRI) and optical imaging modalities [Yang *et al.* (2009)]. MRI delivers the information about the anatomical and physiological information with high resolution while optical imaging offers rapid screening. Subsequently, Srivastava *et al.* reported the multimodal bioimaging application of CQDs from the iron oxide doped CQDs (IO-CQDs) [Srivastava *et al.* (2012)]. Lately, several research groups are getting involved the the potential application of CQDs in a cell imaging agent [Cao *et al.* (2007), Hsu *et al.* (2013), Singh *et al.* (2019)]. It is also observed that the cellular imaging application is highly influenced by temperature, and found that at 48 °C, temperature CQDs were not internalized into the cells. The translocation of CQDs inside the cell were owed to the endocytosis process as well as coupling of CQDs with membrane translocation peptide overcome the cell membrane barrier and facilitate the translocation process [Santra *et al.* (2005), Stroh *et al.* (2005)]. Thus, it is believed the excellent biocompatibility of CQDs plays an essential role in cell targeting imaging applications.

### 1.5.6. Sensing of pesticides and fungicides

Recently, CQDs have also been used in the detection of pesticides and fungicides. Pesticides and fungicides might present at a low amount in the environmental samples, which caused the human health; hence, required to trace them effectively. In a recent investigation, Li *et al.* have designed N and P co-doped fluorescent CQDs for the detection of carbendazim (a fungicide), which had a very low detection limit of 0.002  $\mu\text{M}$  in a linear range from 0.005–0.16  $\mu\text{M}$  [Yang *et al.* (2018)]. In another study, Li *et al.* prepared N and S co-doped CQDs via pyrolysis of an ionic liquid N-methylethanolammoniumthioglycolate. The synthesized CQDs had efficiently used as a nanoprobe to detect pesticide carbaryl by the use of acetylcholinesterase (AChE) and choline oxidase. In this study, the measured detection limit was very low  $5.4 \times 10^{-9}$  g/L in the concentration range of  $6.3 \times 10^{-9}$  g/L and  $6.3 \times 10^{-4}$  g/L [Li *et al.* (2016)].

### 1.5.7. Biosensor

The sturdy photostability, ease of surface modification, excitation dependent emission, nontoxicity, excellent biocompatibility, good cell permeability, and high water solubility of CQDs deliver an effective and prominent platform for the determination of iron, glutathione, glucose, cellular, potassium, Copper, nucleic acid, and pH [Shi *et al.* (2011), Li *et al.* (2011), Wei *et al.* (2012), Zhao *et al.* (2011)]. The fluorescent labeled single stranded DNA (ss-DNA) was adsorbed on the CQDs surface through the  $\pi$ - $\pi$  interaction resultant to the quenching of fluorescence emission; afterward, ss-DNA bind to a complementary target and hybridized to double stranded DNA (ds-DNA) which detached from the surface of CQDs and fluorescence reappearance was detected [Zhao *et al.* (2011)]. Additionally, CQDs were utilized in detecting bacterial cells in sewage water, small bio-analyte including glutathione,

dopamine, glucose, ascorbic acid, mitochondrial  $H_2O_2$ , antibacterial drugs, and so on [Zheng *et al.* (2013), Niu *et al.* (2014), Mao *et al.* (2012), Huang *et al.* (2013)]. Recently, our research group synthesized  $MnO_2$  based nanocomposite (N,S-CQD- $MnO_2$ ) for the GSH detection [Bano *et al.* (2020)]. The addition of  $MnO_2$  nanosheets quenches the fluorescence emission of CQDs by the phenomenon of fluorescence resonance energy transfer and strong electrostatic interaction between N,S-CQDs and  $MnO_2$ . Further, addition of GSH in the quenched system of N,S-CQD- $MnO_2$  nanocomposite reappeared the fluorescence of CQDs, thus, our designed nano-composite could act as turn-on nanoprobe for the detection of biomolecules GSH. Moreover, fluorescent CQDs can exhibit peroxidase like activity, which has used as a nanoprobe for biomolecule [Jv *et al.* (2010), Gao *et al.* (2017), Jiang *et al.* (2017), Chandra *et al.* (2019)]. Recently, our group synthesized CQDs through the hydrothermal treatment of latexes *Euphorbia milii* (*E. milii*) for the detection of biomolecule GSH. The synthesized CQDs showed peroxidase mimic activity which was used in the colorimetric detection of GSH [Bano *et al.* (2019)]. The feasibility of the proposed sensing system toward GSH was successfully investigated over the real samples as a human blood serums. Besides, the fluorescent CQDs based peroxidase substrate offers an efficient tool for colorimetric and fluorimetric detection of various biologically active molecules such as ascorbic acid, glucose, glutathione, amino acid etc.

#### **1.5.8. Temperature sensor**

In recent years, CQDs have also been utilized in the field of temperature probe. Han *et al.* produced N and S doped co-doped CQDs with blue fluorescence emission and high QY 26.9% by using the precursors sodium citrate and thiourea. These CQDs are used as a temperature detection whose fluorescence emission quenched gradually with the rise in

temperature (5-70 °C) [Han *et al.* (2019)]. Mechanistic study confirmed that quenching of CQDs were probably due to the synergistic effect and aggregation of CQDs with rise in temperature. Similarly, in a recent year, Shi *et al.* synthesized N and S co-doped CQDs as an effective temperature sensor which displayed good temperature-dependent fluorescence emission along with a sensational linear response between 20 and 80 °C [Shi *et al.* (2017)]. Lately, Zuo *et al.* demonstrated that because of prominent temperature dependence of the fluorescence emission spectra, the synthesized N and S co-doped CQDs can work as versatile nanothermometry devices by the use of the sensitive temperature range from 5 to 80 °C [Zuo *et al.* (2019)].

#### **1.5.9. Sensing of heavy metal ions**

Heavy metal pollution has become a major worldwide concern for years because of severe risks in the environment and the human health. The most common heavy metals are copper, chromium, cadmium, arsenic, mercury, lead, cobalt, nickel, and zinc [Lambert *et al.* (2000)]. The contamination of these heavy metals in water bodies and soil occur due to natural means such as natural weathering of the earth crust, volcanic eruption, soil erosion, earthquake as well as human activity including sewage discharge, mining, industrial effluents, urban runoff, insect controlling chemical agent and many others [Morais *et al.* (2012)]. The conventional techniques such as polarography, auger electron spectroscopy (AES), high performance liquid chromatography (HPLC), and inductively coupled plasma mass spectroscopy (ICPMS) comprise the use of sophisticated and expensive instrumentations, which limit their realistic applicability [Lu *et al.* (2012), Contino *et al.* (2016), Zhang *et al.* (2012), Sakamoto-Arnold *et al.* (1987), Yao *et al.* (2010), Mehta *et al.* (2013)]. Therefore, it is an urgent need to develop an efficient analytical method for the

detection of these metal ions. Recently, CQDs have materialized in the precise optical sensor systems based on absorption and fluorescence phenomenon along with the detection limit in the range of nanomolar (nM), picomolar (pM), or femtomolar (fM). Due to the advantages of ease of synthesis, economical methodologies, easy functionalization, relatively high fluorescence QY, high photostability, and low cyto-toxicity, CQDs could be used in the sensing applications.

#### 1.5.9.1. Hg (II) sensing

Mercury is one of the most toxic pollutants with the feature of substantial toxicity. It can be bioaccumulated in the human body and other flora and fauna which can cause serious health ailments even at low concentrations such as expiratory dyspnoea, headaches, stomach perforation, renal failure hyperspasmia, and so on [Gajalakshmi *et al.* (2012), Flora *et al.* (2008)]. Therefore, it is essential to detect these ions specifically with high sensitivity. Recently, doped/undoped CQDs become a promising candidates to detect these  $\text{Hg}^{2+}$  ions in a different conditions. In particular, the CQDs-based nanosensor is very simple, rapid, inexpensive, and environmentally friendly. In an investigation, Yuan *et al.* have proposed a turn-on fluorescence nanosensor toward  $\text{Hg}^{2+}$  detection [Yuan *et al.* (2014)]. In this work, blue emitting CQDs were produced by pyrolyzing the mixture of TTDDA and citric acid in glycerol. The fluorescence of the synthesized CQDs was quenched after conjugating with bis(dithiocarbamate)copper(II). In this study, fluorescence quenching of CQDs was due to the electron transfer and energy transfer phenomenon; though, the addition of  $\text{Hg}^{2+}$  inhibits the energy transfer, leads to the fluorescence recovery of CQDs. Thus, CQDs worked as a turn-on sensor with the detection limit of 4 ppb. The feasibility of the proposed sensing system was successfully applied to tap water, lake water, and urine sample with excellent

recovery. In an investigation, Zhang *et al.* synthesized blue-emitting N-doped CQDs along with QY of 15.7%. The CQDs were produced by the use of folic acid (carbon and nitrogen precursors) through the hydrothermal process, which has provided as an efficient platform for label-free sensitive detection of  $\text{Hg}^{2+}$  ions with LOD of 0.23  $\mu\text{M}$  [Zhang *et al.* (2014)]. Also, the N-CQDs-based  $\text{Hg}^{2+}$  ions sensor has successfully applied to the determination of  $\text{Hg}^{2+}$  in real lake water and tap water samples. In a recent study, our group synthesized CQDs based nanoprobe for the detection of  $\text{Hg}^{2+}$  [Bano *et al.* (2018)]. In this work, CQDs were prepared through the hydrothermal treatment of *Tamarindus indica* leaves (*T. indica*) with high fluorescence QY of 46.6%. The feasibility of the proposed sensing system was successfully checked in a pond water sample as a real sample analysis.

#### 1.5.9.2. Fe (III) sensing

Ferric ion ( $\text{Fe}^{3+}$ ) is almost a ubiquitous metal ion in biological and environmental systems. Zhu *et al.* designed CQDs based nanoprobe to detect  $\text{Fe}^{3+}$  along with a detection limit of 0.55 ppm. This sensing system was based on the specific interaction amid  $\text{Fe}^{3+}$  and phenolic hydroxyl groups [Yang *et al.* (2014)]. In addition, Chen *et al.* designed an N-doped CQDs for detecting the ferric ions which had a detection limit of 2.5 nM [Chen *et al.* (2014)]. Afterthat, Chandra *et al.* reported highly fluorescent nitrogen and phosphorus co-doped CQDs which was applied in the determination of  $\text{Fe}^{3+}$  in cancer cells. This sensing system was based on the measuring of quenching variation [Chandra *et al.* (2016)]. In another literature, Li *et al.* synthesized label free  $\text{Fe}^{3+}$  probe by using N-doped CQDs with the detection limit of 0.001 M [Xu *et al.* (2017)]. Recently, our research group also synthesized CQDs based nanoprobe for the detection of  $\text{Fe}^{3+}$  through one pot hydrothermal treatment of *Artocarpus lakoocha*. This sensing system was based on the quenching mechanism with the

detection limit 0.62  $\mu\text{M}$ . The practical feasibility of the proposed sensing system was further investigated in the real samples investigation as river water and human blood serum samples [Yadav *et al.* (2019)].

### 1.5.9.3. Cr (VI) and Cr (II) sensing

Chromium (VI) [Cr (VI)] and chromium (II) [Cr (II)] are highly toxic and more carcinogenic to human health in comparison to other oxidation states Cr (0), and Cr (III) metal ions due to wide use and constant release. Thus, tracing these ions in environmental samples are highly demanded up to the micromolar level. Lately, doped or codoped CQDs have been widely used for monitoring these ions efficiently. In an investigation, Zheng *et al.* have synthesized N-doped CQDs to design “On-Off” fluorescent nanoprobe for detecting Cr (VI) which was based on the inner filter effect (IFE), since absorption spectrum of Cr (VI) covered the emission and excitation of fluorescent CQDs [Zheng *et al.* (2013)]. Similarly, Singh *et al.* synthesized N and P doped CQDs and they have acted as a nanoprobe for the selective and sensitive detection of Cr (VI). In this study, the sensing system was based on the inner filter effect and static quenching mechanism between Cr (VI) and N,P-CQDs and in this process Cr (VI) reduced to less hazardous lower valent Cr (III) species [Singh *et al.* (2018)]. Analogously, Omer *et al.* synthesized N and P co-doped CQDs that displayed high selectivity for the detection of chromium (II) ions via quenching mechanism. The designed CQDs-based nanoprobe had high sensitivity along with LOD of 0.1  $\mu\text{M}$  in a linear concentration range of 0.5–1.3  $\mu\text{M}$  [Omer *et al.* (2019)].

#### 1.5.9.4. Co (II) sensing

Cobalt plays a vital role in the functioning of the human body mainly in the nourishment of red blood cells (RBC's) and the preservation of nerve cells. Therefore, the development of rapid, reliable, non-costly, and selective detection of cobalt is highly demanded upto the micromolar level. Recently, CQDs have been efficiently used for the detection of  $\text{Co}^{2+}$ . In an investigation, Chang *et al.* stated a CQDs based nanoprobe for the detection of  $\text{Co}^{2+}$  via direct and simple quenching mechanism. The mechanistic study confirmed that the cobalt ions reacted with cysteine on the CQDs surface to form a  $\text{Co}_x\text{S}_y$  compounds, which caused the fluorescence quenching. In this study, the measured detection limit was 5 nM in the linear range from 10 nM to 100 mM [Cheng *et al.* (2015)]. Recently, our group synthesized N-doped CQDs for the detection of  $\text{Co}^{2+}$ . In this study, N-CQDs were synthesized via the hydrothermal treatment of glycine and polyethyleneimine. The measured detection limit was 0.12 mM which was below the permissible limit in vitamin B-12 ( $1 \times 10^{-3}$  mM) [Bano *et al.* (2019)].

#### 1.6. Motivation of the study

Most of the synthetic methods were reported based on the Top-down and Bottom-up approaches from the various organic precursors. Though, the top down techniques have some limitation as it involved the use of massive precursors, complex synthetic procedures and requirement of high purification cost. Meanwhile, the bottom-up techniques involved the use of small organic precursors. Nevertheless, most of the methods suffer some issues such as low fluorescent quantum yield, post surface passivation, multistep synthesis method, and time consuming process. After intensive observation of these limitations an effort has been emphasized in synthesizing fluorescent CQDs up to high fluorescence quantum yield by the

use of bottom-up approach through the hydrothermal method from the various chemical and natural organic precursors. It is a one-step synthesis method and no requirement of post passivation. In addition, the hydrothermal method provides several advantages over other method including, it is ecofriendly, nontoxic, economical and less time consuming. Successively, the synthesized CQDs are exploited in designing sensing applications.

### 1.7. Research Objectives

From the careful literature survey and abovementioned background information this research work purposes in synthesizing CQDs and exploits for the sensing application via the fluorimetric and colorimetric method. Thus, the main objectives of the present research work are as follow:

- To synthesize CQDs with high fluorescence quantum yield from the various chemical as well as natural organic precursors by the use of the one-step hydrothermal approach.
- To characterize these fluorescent materials by the use of various instrumentation techniques such as:
  - ❖ Fourier Transform infrared spectroscopy (FTIR)
  - ❖ X-Ray Photoelectron Spectroscopy (XPS)
  - ❖ UV-visible spectroscopy
  - ❖ Fluorescence spectroscopy
  - ❖ Time resolved fluorescence life time spectroscopy
  - ❖ Transmission Electron Microscopy (TEM)
  - ❖ X-Ray Diffraction Spectroscopy (XRD)

- To design CQDs based nanoprobe for the detection of heavy metal ions such as Co (II) and Hg (II) and bioactive molecule glutathione (GSH).
- To explore the potential feasibility of our designed nanoprobe in a real natural sample analysis.